Temporal variations of perfluoroalkyl substances partitioning between surface water, suspended sediment, and biota in a macrotidal estuary

Gabriel Munoz, Hélène Budzinski, Marc Babut, Jérémy Lobry, Jonathan Selleslagh, Nathalie Tapie, Pierre Labadie

Temporal variations of perfluoroalkyl substances partitioning between surface water, suspended sediment, and biota in a macrotidal estuary

Gabriel Munoz[a], Hélène Budzinski[b], Marc Babut[c], Jérémy Lobry[d], Jonathan Selleslagh[d], Nathalie Tapie[a], and Pierre Labadie[b,*]

[a]: Université de Bordeaux, EPOC, UMR 5805, LPTC Research Group, 33400 Talence, France.

[b]: CNRS, EPOC, UMR 5805, LPTC Research Group, 33400 Talence, France.

[c]: UR MALY Irstea, 69626 Villeurbanne cedex, France.

[d]: IRSTEA, UR EABX, 33610 Cestas, France.

*Corresponding author.

Contact: pierre.labadie@u-bordeaux.fr

Published in Chemosphere (June 2019), DOI: 10.1016/j.chemosphere.2019.05.281

Graphical abstract

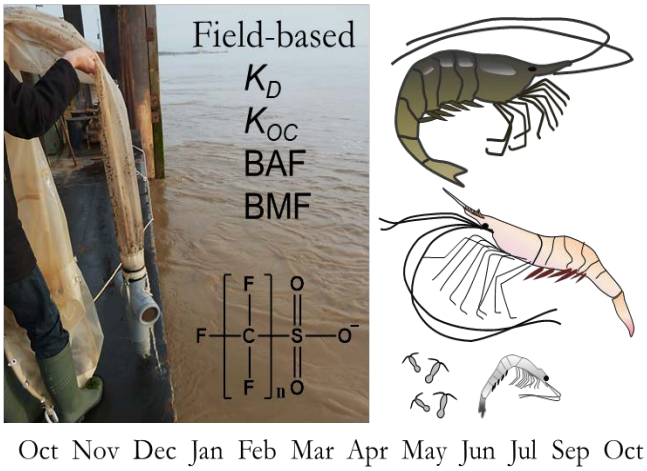

Highlights

- A temporal follow-up of PFAS partitioning was conducted in a macrotidal estuary.
- Mean ΣPFASs = 6.5 ng L^{-1} in water, 3 ng g^{-1} in SPM, and 6.4 ng g^{-1} in invertebrates.
- PFAS levels and profiles were relatively stable across different seasons.
- Chain length was the key controlling factor of PFAS sorption and bioaccumulation.
- Partitioning coefficients and bioaccumulation factors varied within a limited range.

Abstract

A one-year monitoring study was conducted in a macrotidal estuary to assess the temporal variations and partitioning behavior of perfluoroalkyl and polyfluoroalkyl substances (PFASs). Surface water, suspended particulate matter (SPM), and invertebrates including zooplankton (copepods, mysids) and shrimps were sampled on a monthly basis in the Gironde Estuary (SW France). Environmental parameters such as suspended solid loads, salinity, and river water flow rate were highly variable at the study site. However, moderate seasonal variations were observed in terms of PFAS levels and profiles. Summed PFAS (Σ_{22}PFAS) concentrations averaged 6.5 ± 2.7 ng L^{-1} in the dissolved phase and 3.0 ± 1.2 ng g^{-1} dry weight in the SPM. The Σ_{22}PFAS was in the range of 1.7–13 ng g^{-1} wet weight in invertebrates. C_5–C_8 perfluoroalkyl carboxylates (PFCAs) generally prevailed in the dissolved phase, while perfluorooctane sulfonate (PFOS) was dominant in the SPM and biota. Suspended sediment-water partitioning coefficients Log K_D and Log K_{OC} were correlated with the perfluoroalkyl chain length, as were the particle-bound fraction and bioaccumulation factors (Log BAF). Compound-specific Log BAFs varied within a limited range over the period surveyed. Biomagnification factors (mysids/copepods) were consistently >1 for PFOS, perfluorooctane sulfonamide, and long-chain PFCAs (perfluorodecanoate and perfluorododecanoate), suggesting biomagnification at the base of the estuarine food web.

Keywords

PFASs – Seasonal variations – Suspended sediment – Zooplankton – In situ partitioning – Bioaccumulation

1. Introduction

Perfluoroalkyl and polyfluoroalkyl substances (PFASs) are highly fluorinated chemicals used in a variety of applications and consumer products (Robel et al. 2017; Tokranov et al. 2018), which can result in their emission to the environment (Wang et al. 2017). Due to concerns on environmental and health impacts of PFASs, monitoring surveys have assessed the extent of contamination of aquatic ecosystems (Lindim et al., 2015; Campo et al., 2016; Loos et al., 2017) and water sources (Hu et al., 2016; Boone et al., 2019). Certain PFASs such as perfluorooctane sulfonate (PFOS) are found at widespread scale, including in the open ocean and polar regions (Yeung et al., 2017; Rigét et al., 2019).

The long-chain perfluoroalkyl carboxylates (PFCAs) and perfluoroalkane sulfonates (PFSAs) are of particular concern due to persistent, toxic, and bioaccumulative properties (Gomis et al., 2018; Shi et al., 2018). In homologous series of PFCAs and PFSAs, the logarithm of the bioaccumulation factor (Log BAF) and the number of perfluoroalkyl carbon atoms were shown to be linearly correlated over a certain chain length range (Hong et al., 2015; Kwadijk et al., 2010; Xu et al., 2014). The perfluoroalkyl chain length was also suggested as a key controlling factor of PFCA and PFSA sorption onto sediment or suspended particulate matter (SPM) (Ahrens et al., 2010; Labadie and Chevreuil, 2011a; Zhang et al., 2012).

Significant progress has been achieved in recent years to elucidate the environmental fate of PFASs, but there still exist significant data gaps regarding their temporal dynamics in aquatic ecosystems. Hitherto, temporal surveys of biota have essentially focused on long-term and inter-annual variations, over typically 20–30 years (e.g., Kratzer et al., 2011; Rigét et al., 2013). Inter-annual studies are of fundamental interest to evaluate the impact of recent regulations implying restrictions on C_8-based PFASs use, commerce, and/or production. Besides, seasonal surveys can provide insightful knowledge on the variability of PFAS levels and profiles at smaller time

scales. Available data on intra-annual variability of PFASs remain, however, limited (Cai et al., 2018; Chen et al., 2017; Kong et al., 2018; Pignotti et al., 2017; Zhao et al., 2015).

Although PFAS partitioning studies and biomonitoring surveys have been conducted, few were spatially or temporally integrated (i.e., realized at the exact same place and time period, respectively) or repeated in time to account for temporal variability (Labadie and Chevreuil, 2011b; Powley et al., 2008). Deriving partitioning coefficients from a limited number of field replicates can provide useful preliminary data regarding the environmental fate of pollutants, but there are some caveats. Not accounting for temporal variability may raise questions on the level of representativeness of the reported partitioning coefficients. In estuarine ecosystems, for instance, biogeochemical parameters can greatly vary both spatially and temporally (Sottolichio and Castaing, 1999; Selleslagh et al., 2012). Such variations may, in turn, lead to non-negligible fluctuations in the field partitioning of contaminants. Certain endpoints can have a direct bearing on chemical substances management (e.g., REACH criterion for very bioaccumulative substances: BAF >5000) as well as on the management of water bodies (e.g., environmental quality standards set by the E.U. Water Framework Directive). The variability of *in situ* partitioning should, therefore, be accounted for to make well informed decisions.

In this study, we set out to evaluate the temporal variations of PFAS levels and partitioning behaviors. A one-year monitoring survey was launched on a monthly basis at a single study-site within a highly turbid macrotidal estuary. The specific objectives of the present study were as follows: i) examine potential seasonal variations in PFAS levels and profiles in a highly turbid environment; ii) investigate the partitioning behavior of selected PFASs between abiotic and biotic compartments; and iii) conduct a preliminary assessment of PFAS biomagnification at the base of the estuarine food web.

2. Materials and methods

2.1. Chemicals and standards

A full list of chemicals and solvents is provided in the Supporting Information (SI). Analyte names, acronyms, and structures are also provided in the SI (**Table S1**). Certified PFAS native compounds and isotope-labeled internal standards were all purchased from Wellington Laboratories, Inc. (BCP Instruments, Irigny, France). The targeted PFASs included PFCAs (PFBA, PFPeA, PFHxA, PFHpA, PFOA, PFNA, PFDA, PFUnDA, PFDoDA, PFTrDA, and PFTeDA), PFSAs (PFBS, PFHxS, PFHpS, L-PFOS, and PFDS), perfluorooctane sulfonamide (FOSA) and N-alkylated related compounds (MeFOSA, EtFOSA), N-alkylated perfluorooctane sulfonamide acetic acids (MeFOSAA, EtFOSAA), and 6:2 fluorotelomer sulfonate (6:2 FTSA). Note that in this paper, "PFOS" refers to the sum of the linear (L-PFOS) and branched (Br-PFOS) isomers. $^{13}C_2$-PFHxA $^{13}C_4$-PFOA, $^{13}C_2$-PFDA, $^{13}C_2$-PFUnDA, $^{13}C_2$-PFDoDA, $^{18}O_2$-PFHxS, $^{13}C_4$-PFOS, d_3-N-MeFOSAA, $^{13}C_8$-FOSA, d_3-N-MeFOSA, d_5-N-EtFOSA and $^{13}C_2$-6:2 FTSA were the internal standards used in the present study.

2.2. Study site and sample collection

At the northernmost tip of the Aquitaine coastline, the Gironde estuary (SW France) is a macrotidal estuary resulting from the confluence of the Garonne and Dordogne rivers, the combined flows of which feed into the estuary at Bec d'Ambès (SI **Fig.S1**). The Gironde flows over 70 km in a general northwestern direction through landscapes alternating natural wilderness, small municipalities, and agricultural areas, before entering the Bay of Biscay near Le Verdon. The Gironde is characterized by a fairly permanent maximum turbidity zone, resulting from the mixing of fresh water inflows (from the Garonne and Dordogne rivers and smaller tributaries) and saltwater wedges from incoming tides (Sottolichio and Castaing, 1999). This estuary is of great ecological

value, being an important transit point for several diadromous fish and a nursery area for numerous marine fish during their juvenile stage (Lobry et al., 2008).

The temporal survey was carried out on a monthly basis from October 2012 to October 2013 at Pauillac (Gironde, France). Located on the left-side bank of the Gironde estuary, the municipality lies approximately 20 km downstream from the confluence of the Garonne and Dordogne rivers and 50 km upstream from the mouth of the estuary (SI **Figure S1**). Sample collection was carried out at a pier exterior to the marina (Latitude 45.19845°D, Longitude -0.74259°D) during the last two hours of the rising tide, at dates selected for medium tidal coefficients (mean: 55 ± 8) as described by Tapie (2006). Physical chemical parameters such as water temperature, pH, or salinity were measured on site (SI **Table S2**).

Water sampling was conducted at high tide, using a 1 L high density polyethylene bottle rinsed 3 times with the site surface water prior to sampling and storage in a cooling box. Upon arrival at the laboratory, the water samples were passed through GF/F (0.7 µm) Whatman glass microfiber filters (previously baked at 400°C for 6h and weighed) using Nalgene® polyethylene filtration units. The filtrate was stored at -20°C until analysis. Filters were freeze-dried (24 h) and weighed (to determine the suspended solid amount) prior storage at -20°C until analysis.

A cone-shaped WP-2 net (mesh: 200 µm) was deployed to collect the organisms considered in this study, starting two hours before high tide. Every 5-10 minutes, the net was hauled in and emptied above stacked sieves (mesh sizes: 2 mm, 500 µm and 200 µm). White shrimp (*Palaemon longirostris*), brown shrimp (*Crangon crangon*), and mysids (*Mysidacea, ind.*) were collected and sorted out in the field. Following sacrifice, the catch was stored in 50 mL polypropylene centrifuge tubes. Any other species were returned immediately to the water. Copepods (*Copepoda, ind.*) were preserved in a 10 L bottle containing water from the estuary. In the laboratory, the copepod catch was poured in 4 L glass beakers and mixed (1:1 v/v) with Volvic spring water adjusted to

the adequate salinity (Tapie, 2006). After the decantation of particles and dead animals, live copepods were retrieved from the medium and left overnight in 4 L glass beakers containing Volvic spring water (adjusted to the adequate salinity) and equipped with submerged aerators and an overhanging light source. Particle-free copepods were finally recovered in the 200 µm mesh and stored in 15 mL polypropylene centrifuge tubes. Biota samples were freeze-dried (72 h) and finely ground with pestle and mortar.

2.3. Sample extraction and instrumental analysis

Internal standards were added to the samples at the beginning of the extraction procedure (50 µL of a 20 ng mL^{-1} internal standard mix in methanol). The extraction methods for water and biota samples are described elsewhere (Munoz et al., 2015; Munoz et al., 2017a). Briefly, water samples (1 L) were concentrated using solid phase extraction on Strata X-AW cartridges (200 mg/6 mL), while biota samples [0.25 g dry weight (dw)] underwent a microwave extraction with MeOH prior to Strata X-AW (200 mg/6 mL) and ENVI-Carb graphite (250 mg/6 mL) clean-up. Suspended particulate matter (SPM) samples were extracted by microwave extraction with MeOH, followed by ENVI-Carb graphite (250 mg/6 mL) clean-up. The resulting extracts were concentrated to 300 µL under a nitrogen stream and moderate heating (42 °C), and transferred into polypropylene injection vials for analysis.

PFASs were analyzed by high-performance liquid chromatography coupled to tandem mass spectrometry (HPLC-MS/MS) through a negative electrospray ionization source. A Zorbax Eclipse Plus C18 column (2.1 mm x 100 mm; 1.8 µm particle size) thermostated at 35 °C was used for analyte separation, while a Zorbax SB C18 column (2.1 mm x 30 mm; 3.5 µm particle size) was used as a trap column. HPLC mobile phases were as follows: (A) Milli-Q water with 2 mM ammonium acetate; (B) acetonitrile/Milli-Q water (95:5 v/v) with 2mM ammonium acetate. The injection volume was set at 5 µL and the mobile phase flow rate at 500 µL min^{-1}. The Agilent 1200

LC system was interfaced with an Agilent 6460 triple quadrupole mass spectrometer (Agilent Technologies, Massy, France). Further details on HPLC gradient programs and compound-dependent MS/MS acquisition parameters are provided elsewhere (Munoz et al., 2015).

2.4. Quality assurance and quality control

Method performance was evaluated through the analysis of replicate (n = 3) spiked samples. Spike recoveries were in the range of 53–115% for Vittel mineral water, 60–119% for reference sediment (surrogate for SPM), and 52–119% for brown trout filets from the Kerguelen archipelago (Southern Ocean). Suitable whole-method precision was obtained, with relative standard deviations (RSD) below 25% (SI **Table S3**).

In addition, a non-spiked reference matrix (NIST SRM 1947 Lake Michigan Fish Tissue) was analyzed in parallel to the samples to evaluate method trueness. The values determined for PFOS were between 79–96% of those of NIST or Environment Canada (Reiner et al., 2012), with suitable precision (SI **Figure S2**).

Instrumental blanks remained free of analytes and ISs. Procedural blanks were performed with 0.5 L of Vittel spring water for water samples and with 10 mL of MeOH for SPM and biota samples, submitted to their respective procedures (SI **Table S4**). Limits of detection (LODs) were in the range of 0.002–0.15 ng L^{-1}, 0.001–0.13 ng g^{-1} dw, and 0.001–0.10 ng g^{-1} ww for surface water, SPM, and biota samples, respectively.

R (R version 2.15.3, R Core Team, 2013) and Sigmaplot™ 12.5 (Systat Software) softwares were used to conduct data analysis. Correlations between PFAS levels in the water column and relevant environmental parameters were investigated through the calculation of Spearman's rank order coefficients. Statistical significance was set at $p<0.05$.

3. Results and discussion

3.1. Seasonal variability of hydro-physical parameters

Water temperatures ranged from 6.6–8.7°C during winter months to 19–25.7°C during summer months. The estimated water flow rate at Pauillac ranged from 170 to 4,700 $m^3 s^{-1}$ over the overall study period (SI **Figure S3**) and from 251 to 1,847 $m^3 s^{-1}$ for the specific days of sampling (SI **Table S2**). The lowest salinities were observed from January to June (0–2.7‰) under high flow rate conditions, while the highest salinities (4.5–11.6‰) were observed from July to December (SI **Figure S4**). There was no clear seasonal pattern for the SPM, which was subject to wide variations (130–1,900 mg L^{-1}).

3.2. Seasonal variations of PFAS levels and profiles in the water column

In surface water (dissolved phase), C_5–C_{10} PFCAs, PFBS, PFHxS, and PFOS displayed the highest detection frequencies (100%) (**Table 1**). The 6:2 fluorotelomer sulfonate (6:2 FTSA) was also recurrently detected (75%). Occurrence data are in agreement with a 2014 survey conducted at large spatial scale in this estuary (Munoz et al. 2017b). The median ∑PFASs was 6.2 ng L^{-1}, close to the 7.9 ng L^{-1} median reported at French nationwide scale for 133 rivers and lakes (Munoz et al., 2015). Summed PFAS levels varied up to a factor of 3x, between 3.5 ng L^{-1} (March 2013) and 11 ng L^{-1} (December 2012). Dissolved PFAS levels are relatively stable (**Figure 1a**), compared to some other riverine hydrosystems in France (Labadie and Chevreuil, 2011b). This might be due to a “buffering effect” of riverine inputs through estuarine mixing processes, associated with relatively long water residence times in the estuary (~ 20–85 days) (Castaing and Jouanneau, 1979). The PFAS molecular pattern was dominated by C_5–C_8 PFCAs, PFHxS,

and PFOS with limited variations across the time period of this study, each group accounting respectively for 47±12%, 14±3%, and 17±5% of the summed PFAS levels (**Figure 1b**).

We observed a median dissolved PFOS concentration in surface water of 1.1 ng L^{-1} (mean = 1.04 ± 0.33 ng L^{-1}, range: 0.48–1.6 ng L^{-1}), a relatively low level compared to some major hydrosystems worldwide (Pan et al., 2018). The median PFOS level in the present survey is also about 20 times lower than that in the Seine River downtown Paris (Labadie and Chevreuil, 2011b). The relatively lower PFOS concentrations may be due to higher dilution capability, lower urban and industrial inputs compared to the Paris region, and much higher SPM loads acting as a sink for long-chain PFASs.

The fluctuations of ΣPFASs and compound-specific abundance in the suspended sediment are shown in **Figure 2**. The PFAS concentrations in SPM samples varied by less than one order of magnitude (up to 4.3x) during the present study (ΣPFASs range: 1.3–5.6 ng g^{-1} dw; median = 2.7 ng g^{-1} dw) (**Figure 2a**). The congener profiles also remained consistent during the time period of this study (**Figure 2b**). PFOS was the predominant compound, at 58±7% of ΣPFASs on average. Of these, nearly 70% could be attributed to the linear isomer, in agreement with the distribution of PFOS isomers in sediments and likely reflecting both historical electrofluorination sources and the higher sediment-water partition coefficient (K_D) of L-PFOS (Houde et al., 2008; Labadie and Chevreuil, 2011b).

In the water column (dissolved phase + SPM), PFCAs and PFOS levels were highly correlated to each other and to ΣPFASs (SI **Table S5**). In contrast, 6:2 FTSA was related in a negative fashion to ΣPFASs, suggesting particular sources and/or different environmental fate. The presence of 6:2 FTSA has been linked with industrial locations and firefighting foam impacted sites, for instance via the degradation of precursors to 6:2 FTSA present in aqueous film-forming foam formulations (D'Agostino and Mabury, 2017; Dauchy et al., 2017; Field and Seow, 2017). In

addition, 6:2 FTSA itself could be biotransformed to fluorotelomer unsaturated carboxylates and PFCAs (Zhang et al., 2016; Shaw et al., 2019).

Dissolved PFOS or PFCA levels were not significantly correlated to daily flow rate, which differs from previous observations in the river Seine (Labadie and Chevreuil, 2011b). This indicates that inputs from diffuse sources such as atmospheric deposition may be important compared to those of point sources in this estuary. ΣPFASs was correlated to monthly rainfall (Spearman's rho = 0.58), as were short-chain PFCAs (Spearman's rho = 0.55), which seems to substantiate the prevalence of diffuse sources. The examination of PFHpA/PFOA ratios in the dissolved phase revealed higher values from July to October (1.02–1.35), months that displayed the highest rainfall to flow rate ratios (SI **Figures S5-S6**). According to literature precedent, this may indicate an increase of the relative importance of atmospheric wet deposition at these sampling dates (Simcik and Dorweiler, 2005). Conversely, PFHpA/PFOA ratios decreased in the narrow range of 0.45–0.51 from February to April—a potential outcome of the dilution of atmospheric inputs under high river flow conditions.

3.3. SPM-water partitioning

K_D values were determined by dividing the PFAS concentration in the SPM (in ng kg^{-1} dw) by that of the dissolved phase (in ng L^{-1}), when the analyte was found in both matrices. The average Log K_D was in the range of 2.0–3.8 for C_7–C_{11} PFCAs and 1.9–3.4 for C_6–C_8 PFSAs (**Table 2**). Log K_D values varied within a rather limited range at the water year scale. For instance, the Log K_D of L-PFOS averaged 3.3±0.2 (range = 3.1–3.8), and that of PFOA was 2.4±0.2 (range = 2.2–2.7) (SI **Figure S7**).

The sediment organic carbon–partitioning coefficient (K_{OC}) was derived from the K_D value and SPM organic carbon fraction, f_{oc} (range: 1.6–2.7%). Average Log K_{OC} was in the range of 3.6–5.2 for the compounds considered (**Table 2**).

The particle-related PFAS fraction (φ) was determined by dividing the PFAS concentration in the SPM by that in the water column (i.e., dissolved phase + SPM). For PFSAs, φ varied from 6.5±2% for PFHxS to 62±14% for L-PFOS (**Figure 3**). For PFCAs, φ increased with perfluoroalkyl chain length (power law fitting, SI **Figure S8**), concurring with previous observations by Ahrens et al. (2010) in the Tokyo Bay. Relatively higher φ values were observed in our case. For instance, the φ value of PFDA was in the range of 50–87% in the Gironde estuary, compared to 23±5.7% in Tokyo Bay (Ahrens et al., 2010). This may be related to the much higher suspended solid concentrations than those reported in the Tokyo Bay (130–1900 *vs.* 3–5 mg L^{-1}). Other potentially influencing parameters of the suspended sediment-water partitioning of PFASs include sorbent characteristics (e.g., geochemical composition of the SPM, especially organic carbon content) and water quality parameters (Higgins and Luthy, 2006; Jeon et al., 2011).

3.4. Bioaccumulation and biomagnification

In invertebrates, the mean ΣPFASs [in ng g^{-1} wet weight of the whole body (ww w-b)] was as follows: copepods (2.9±0.8 ng g^{-1} ww w-b); mysids (7.2±2.0 ng g^{-1} ww w-b); white shrimps (4.5±1.2 ng g^{-1} ww w-b); brown shrimps (11±2 ng g^{-1} ww w-b). These levels fall in the same order of magnitude as those observed by Loi et al. (2011) in Mai Po Marshes (Hong Kong) for zooplankton and shrimps (~3–4 ng g^{-1} ww w-b).

Seasonal variations of ΣPFASs for copepods and mysids are shown in the SI (**Figure S9**). Over the time period of this study, ΣPFASs varied only up to a factor of 2.5x for zooplankton and 2.3x for shrimps, further suggesting the relative stability of PFAS levels in this ecosystem. The

increasing ΣPFAS trend observed for mysids in the spring-summer months may be attributed to the increase in prey density (i.e., copepods). In addition, shifts in mysid communities from *Neomysis integer* to *Mesopodopsis slabberi* typically occur from April to August (David et al., 2005). Grazing of vegetal particulate organic matter or periphyton may be another key PFAS exposure route for mysids in the spring-summer months, especially for *Mesopodopsis slabberi* – *Neomysis integer* being rather carnivorous and feeding primarily on copepods in the Gironde estuary (David et al., 2006).

In zooplankton, PFOS dominated the PFAS pattern (SI **Figure S10**). The mean contribution of PFOS to the ΣPFASs was 56±7 % for copepods and 60±8 % for mysids. This agrees with observations by Loi et al. (2011) who reported a mean PFOS abundance of ~57% for zooplankton. Interestingly, FOSA was the dominant congener in white shrimps, followed by PFOS (35±5 and 30±8 % of ΣPFASs, respectively). The distinctive PFAS pattern observed in shrimps may be a consequence of a low metabolic capacity to transform FOSA and FOSA-like compounds to PFOS. Another indication to support this hypothesis is the relatively high abundance observed for N-alkylated perfluorooctane sulfonamide acetic acids (~9% of ΣPFASs) in shrimps (SI **Figure S10**). Tomy et al. (2004) also reported EtFOSA concentrations greatly exceeding those of PFOS for shrimps (*Pandalus borealis* and *Hymenodora glacialis*) from an Eastern Arctic marine food web. The biotransformation of other perfluorooctanesulfonamide-based PFASs (not targeted in the present survey) could also have played a role in the observed FOSA levels (Mejia-Avendaño et al. 2016; Barzen-Hanson et al. 2017).

When applicable, bioaccumulation factors (BAFs) were calculated as the ratio of the concentration in biota (ng kg^{-1} ww) to that in the water (ng L^{-1}) (dissolved phase) for each species and each sampling date (**Table 2**). Mean Log BAFs were generally comparable in zooplankton and shrimps, in contrast to observations from Taihu Lake (China) where Log BAFs were ~0.6–1.6 log units higher in shrimps than in zooplankton (Xu et al., 2014). An illustration of the year-round variations

of Log BAFs for PFOS, PFNA, and FOSA is provided in **Figure 4**. Log BAFs remained relatively constant, suggesting that PFAS concentrations in zooplankton and nekton were under near-equilibrium conditions with those in the dissolved phase.

Exceedances to the "very bioaccumulative" (vB) criterion set in Annex XIII of REACH (bioconcentration factor > 5,000) were observed for L-PFOS, PFUnDA, and FOSA (mean Log BAF = 3.4–3.9, 3.7–4.1, and 4.1–5.0, respectively) (**Table 2**). Log BAFs increased linearly with increasing perfluoroalkyl chain length, each additional CF_2 moiety contributing to an increase of 0.32–0.44 log units for PFCAs and 0.71–1.0 log units for PFSAs (SI **Figure S11**). These trends are in agreement with observations for other model organisms (Kwadijk et al., 2010; Labadie and Chevreuil, 2011a; Ahrens et al., 2015). Biota to suspended sediment accumulation factors (BSSAF) were in the range of 0.3–29 for the compounds considered (**Table 2**).

Biomagnification factors (BMF = $C_{predator}/C_{prey}$) were tentatively assessed for mysids/copepods (SI **Figure S12**). With the exception of PFHxS, average BMFs were >1, the highest values being reported for L-PFOS and FOSA (3.3±2.1 and 5.2±2.5, respectively). We only observed BMFs consistently >1 [95 % confidence interval ($CI_{95\%}$)] for PFDA ($CI_{95\%}$ = [1.3; 3.5]), PFDoDA ($CI_{95\%}$ = [1.3; 2.2]), Br-PFOS ($CI_{95\%}$ = [1.8; 3.5]), L-PFOS ($CI_{95\%}$ = [2.1; 4.5]), and FOSA ($CI_{95\%}$ = [3.8; 6.6]), suggesting that these compounds may undergo biomagnification at the first trophic levels of the estuarine food web. Such results are consistent with previous findings by Munoz et al. (2017a), who provided evidence for the apparent biomagnification of these PFASs in the Gironde estuary when the whole estuarine trophic web was considered.

4. Conclusions

The present survey explored the year-round variations of a wide range of PFASs in a macrotidal estuary. PFAS levels and profiles varied within a rather limited range over the time period of the study. PFAS concentrations in surface water were not significantly correlated to flow rate, suggesting the prevalence of diffuse PFAS sources at this site. Field-based distribution coefficients (i.e., K_D, K_{OC}, and BAF) were moderately affected by seasonal variations. The magnitude of the suspended solid loads in this highly turbid estuary implies that, in the water column, long-chain perfluoroalkyl carboxylates and sulfonates are mainly bound to the SPM (φ > 60%). From an ecotoxicological standpoint, this could entail different PFAS exposure pathways for organisms dwelling in the maximum turbidity zone of estuaries, for instance via the ingestion of particulate organic matter by deposivores or suspensivores. Biomagnification factors (BMFs mysids/copepods) were consistently >1 (95% confidence interval) for PFOS, FOSA, and certain long-chain perfluoroalkyl carboxylates, suggesting the biomagnification of these compounds at the base of the estuarine food web.

Acknowledgments

This study was carried out within the PFC-Gironde CNRS project (EC2CO-Ecodyn INSU), with financial support from the French National Research Agency (ANR). The study was conducted in the frame of the Investments for the future Program, within the Cluster of Excellence COTE (ANR-10-LABX-45). The authors also acknowledge funding from the Aquitaine Regional Council and the European Union (CPER A2E project and ERDF). The authors wish to thank Virginie Bocquet, Mariange Cornet, Patrick Pardon, Gwenaël Abril, and Dominique Poirier for their contribution. Year-round daily data of salinity and turbidity at Pauillac were supplied by MAGEST (Réseau de surveillance automatisée du système estuarien Garonne–Dordogne–Gironde). IdEx Bordeaux (ANR-10-IDEX-03-02) provided the PhD grant allocated to G. Munoz.

References

Ahrens, L., Taniyasu, S., Yeung, L.W.Y., Yamashita, N., Lam, P.K.S., Ebinghaus, R., **2010**. Distribution of polyfluoroalkyl compounds in water, suspended particulate matter and sediment from Tokyo Bay, Japan. *Chemosphere* 79, 266–272.

Ahrens, L., Norström, K., Viktor, T., Cousins, A.P., Josefsson, S., **2015**. Stockholm Arlanda Airport as a source of per- and polyfluoroalkyl substances to water, sediment and fish. *Chemosphere* 129, 33–38.

Annex XIII of REACH, retrieved at <http://www.reachonline.eu/REACH/EN/REACH_EN/articleXIII.html>.

Barzen-Hanson, K.A., Roberts, S.C., Choyke, S., Oetjen, K., McAlees, A., Riddell, N., McCrindle, R., Ferguson, P.L., Higgins, C.P., Field, J.A., **2017**. Discovery of 40 classes of per-and polyfluoroalkyl substances in historical aqueous film-forming foams (AFFFs) and AFFF-impacted groundwater. *Environ. Sci. Technol.* 51, 2047–2057.

Boone, J.S., Vigo, C., Boone, T., Byrne, C., Ferrario, J., Benson, R., Donohue, J., Simmons, J.E., Kolpin, D.W., Furlong, E.T., Glassmeyer, S.T., **2019**. Per-and polyfluoroalkyl substances in source and treated drinking waters of the United States. *Sci. Total Environ.* 653, 359–369.

Cai, Y., Wang, X., Wu, Y., Zhao, S., Li, Y., Ma, L., Chen, C., Huang, J. Yu, G., **2018**. Temporal trends and transport of perfluoroalkyl substances (PFASs) in a subtropical estuary: Jiulong River Estuary, Fujian, China. *Sci. Total Environ.* 639, 263–270.

Campo, J., Lorenzo, M., Pérez, F., Picó, Y., Farré, M., Barceló, D., **2016**. Analysis of the presence of perfluoroalkyl substances in water, sediment and biota of the Jucar River (E Spain). Sources, partitioning and relationships with water physical characteristics. *Environ. Res.* 147, 503–512.

Castaing, P., Jouanneau, J.M. **1979**. Temps de résidence des eaux et des suspensions dans l'estuaire de la Gironde. *J. Rech. Oceanogr.*, IV, 41-52

Chen, H., Han, J., Zhang, C., Cheng, J., Sun, R., Wang, X., Han, G., Yang, W., He, X., **2017**. Occurrence and seasonal variations of per-and polyfluoroalkyl substances (PFASs) including fluorinated alternatives in rivers, drain outlets and the receiving Bohai Sea of China. *Environ. Pollut.* 231, 1223–1231.

D'Agostino, L.A., Mabury, S.A., **2017**. Certain perfluoroalkyl and polyfluoroalkyl substances associated with aqueous film forming foam are widespread in Canadian surface waters. *Environ. Sci. Technol.* 51, 13603–13613.

Dauchy, X., Boiteux, V., Bach, C., Colin, A., Hemard, J., Rosin, C., Munoz, J.F., **2017**. Mass flows and fate of per-and polyfluoroalkyl substances (PFASs) in the wastewater treatment plant of a fluorochemical manufacturing facility. *Sci. Total Environ.* 576, 5493–558.

David, V., Sautour, B., Chardy, P., Leconte, M., **2005**. Long-term changes of the zooplankton variability in a turbid environment: the Gironde estuary (France). *Estuar. Coast. Shelf Sci.* 64, 171–184.

David, V., Sautour, B., Galois, R., Chardy, P., **2006**. The paradox high zooplankton biomass–low vegetal particulate organic matter in high turbidity zones: What way for energy transfer? *J. Exp. Mar. Biol. Ecol.* 333, 202–218.

Field, J.A., Seow, J., **2017**. Properties, occurrence, and fate of fluorotelomer sulfonates. *Critical Reviews in Environmental Science and Technology* 47, 643–691.

Gomis, M.I., Vestergren, R., Borg, D., Cousins, I.T., **2018**. Comparing the toxic potency in vivo of long-chain perfluoroalkyl acids and fluorinated alternatives. *Environ. Int.* 113, 1–9.

Higgins, C.P., Luthy, R.G., **2006**. Sorption of perfluorinated surfactants on sediments. *Environ. Sci. Technol.* 40, 7251–7256.

Hong, S., Khim, J.S., Wang, T., Naile, J.E., Park, J., Kwon, B.O., Song, S.J., Ryu, J., Codling, G., Jones, P.D., Lu, Y., Giesy, J.P., **2015**. Bioaccumulation characteristics of perfluoroalkyl acids (PFAAs) in coastal organisms from the west coast of South Korea. *Chemosphere* 129, 157–163.

Houde, M, Czub, G., Small, J.L., Backus, S., Wang, X., Alae, M., Muir, D.C.G., **2008**. Fractionation and bioaccumulation of perfluorooctane sulfonate (PFOS) isomers in a lake Ontario food web. *Environ. Sci. Technol.* 42, 9397–9403.

Hu, X.C., Andrews, D.Q., Lindstrom, A.B., Bruton, T.A., Schaider, L.A., Grandjean, P., Lohmann, R., Carignan, C.C., Blum, A., Balan, S.A., Higgins, C.P., **2016**. Detection of poly-and perfluoroalkyl substances (PFASs) in US drinking water linked to industrial sites, military fire training areas, and wastewater treatment plants. *Environ. Sci. Technol. Lett.* 3, 344–350.

Jeon, J., Kannan, K., Lim, B.J., An, K.G., Kim, S.D., **2011**. Effects of salinity and organic matter on the partitioning of perfluoroalkyl acid (PFAs) to clay particles. *J. Environ. Monit.* 13, 1803–1810.

Kong, X., Liu, W., He, W., Xu, F., Koelmans, A.A., Mooij, W.M., **2018**. Multimedia fate modeling of perfluorooctanoic acid (PFOA) and perfluorooctane sulphonate (PFOS) in the shallow lake Chaohu, China. *Environ. Pollut.* 237, 339–347.

Kratzer, J., Ahrens, L., Roos, A., Bäcklin, B.M., Ebinghaus, R., **2011**. Reprint of: Temporal trends of polyfluoroalkyl compounds (PFCs) in liver tissue of grey seals (Halichoerus grypus) from the Baltic Sea, 1974–2008. *Chemosphere* 85, 253–261.

Kwadijk, C.J.A.F., Korytár, P., Koelmans, A.A., **2010**. Distribution of Perfluorinated Compounds in Aquatic Systems in the Netherlands. *Environ. Sci. Technol.* 44, 3746–3751.

Labadie, P., Chevreuil, M., **2011a**. Partitioning behavior of perfluorinated alkyl contaminants between water, sediment and fish in the Orge River (nearby Paris, France). *Environ. Pollut.* 159, 391–397.

Labadie, P., Chevreuil, M., **2011b**. Biogeochemical dynamics of perfluorinated alkyl acids and sulfonates in the River Seine (Paris, France) under contrasting hydrological conditions. *Environ. Pollut.* 159, 3634–3639.

Lindim, C., Cousins, I.T., **2015**. Estimating emissions of PFOS and PFOA to the Danube River catchment and evaluating them using a catchment-scale chemical transport and fate model. *Environ. Pollut.* 207, 97–106.

Lobry, J., David, V., Pasquaud, S., Lepage, M., Sautour, B., and Rochard, E., **2008**. Diversity and stability of an estuarine trophic network. *Mar. Ecol. Prog. Ser.* 35, 13–25.

Loi, E.I.H., Yeung, L.W.Y., Taniyasu, S., Lam, P.K.S., Kannan, K., Yamashita, N., **2011**. Trophic magnification of poly- and perfluoroalkyl compounds in a subtropical food web. *Environ. Sci. Technol.* 45, 5506–5513.

Loos, R., Tavazzi, S., Mariani, G., Suurkuusk, G., Paracchini, B., Umlauf, G., **2017**. Analysis of emerging organic contaminants in water, fish and suspended particulate matter (SPM) in the Joint Danube Survey using solid-phase extraction followed by UHPLC-MS-MS and GC–MS analysis. *Sci. Total Environ. 607*, 1201–1212.

Mejia-Avendaño, S., Vo Duy, S., Sauvé, S., Liu, J., **2016**. Generation of perfluoroalkyl acids from aerobic biotransformation of quaternary ammonium polyfluoroalkyl surfactants. *Environ. Sci. Technol.* 50, 9923–9932.

Munoz, G., Giraudel, J.L., Botta, F., Lestremau, F., Dévier, M.H., Budzinski, H., Labadie, P., **2015**. Spatial distribution and partitioning behavior of selected poly- and perfluoroalkyl substances in freshwater ecosystems: A French nationwide survey. *Sci. Total Environ.* 517, 48–56.

Munoz, G., Budzinski, H., Babut, M., Drouineau, H., Lauzent, M., Menach, K.L., Lobry, J., Selleslagh, J., Simonnet-Laprade, C., Labadie, P., **2017a**. Evidence for the Trophic Transfer of Perfluoroalkylated Substances in a Temperate Macrotidal Estuary. *Environ. Sci. Technol. 51*, 8450–8459.

Munoz, G., Budzinski, H., Labadie, P., **2017b**. Influence of Environmental Factors on the Fate of Legacy and Emerging Per-and Polyfluoroalkyl Substances along the Salinity/Turbidity Gradient of a Macrotidal Estuary. *Environ. Sci. Technol.* 51, 12347–12357.

Pan, Y., Zhang, H., Cui, Q., Sheng, N., Yeung, L. W., Sun, Y., Guo, Y., Dai, J., **2018**. Worldwide distribution of novel perfluoroether carboxylic and sulfonic acids in surface water. *Environ. Sci. Technol.* 52, 7621–7629.

Pignotti, E., Casas, G., Llorca, M., Tellbüscher, A., Almeida, D., Dinelli, E., Farré, M., Barceló, D., **2017**. Seasonal variations in the occurrence of perfluoroalkyl substances in water, sediment and fish samples from Ebro Delta (Catalonia, Spain). *Sci. Total Environ. 607*, 933–943.

Powley, C.R., George, S.W., Russell, M.H, Hoke, R.A. Buck, R.C., **2008**. Polyfluorinated chemicals in a spatially and temporally integrated food web in the Western Arctic. *Chemosphere* 70, 664–672.

Reiner, J.L., O'Connell, S.G., Butt, C.M., Mabury, S.A., Small, J.M., De Silva, A.O., Muir, D.C.G., Delinsky, A.D., Strynar, M.J., Lindstrom, A.B., Reagen, W.K., Malinsky, M., Schafer, S., Kwadijk, C.J.A.F., Schantz, M.M., Keller, J.M., **2012**. Determination of perfluoroalkyl acid concentrations in biological standard reference materials. *Anal. Bioanal. Chem.* 404, 2683–2692.

Rigét, F., Bossi, R., Sonne, C., Vorkamp, K., Dietz, R., **2013**. Trends of perfluorochemicals in Greenland ringed seals and polar bears: Indications of shifts to decreasing trends. *Chemosphere* 93, 1607–1614.

Rigét, F., Bignert, A., Braune, B., Dam, M., Dietz, R., Evans, M., Green, N., Gunnlaugsdóttir, H., Hoydal, K.S., Letcher, R., Muir, D., Schuur, S., Stern, G., Tomy, G., Vorkamp, K., Wilson, S., **2019**. Temporal trends of persistent organic pollutants in Arctic marine and freshwater biota. *Sci. Total Environ.* 649, 99–110.

Robel, A.E., Marshall, K., Dickinson, M., Lunderberg, D., Butt, C., Peaslee, G., Stapleton, H.M., Field, J.A., **2017**. Closing the Mass Balance on Fluorine on Papers and Textiles. *Environ. Sci. Technol.* 51, 9022–9032.

Selleslagh, J., Lobry, J., N'Zigou, A.R., Bachelet, G., Blanchet, H., Chaalali, A., Sautour, B., Boët, P., **2012**. Seasonal succession of estuarine fish, shrimps, macrozoobenthos and plankton: Physico-chemical and trophic influence. The Gironde estuary as a case study. *Est. Coast. Shelf Sci.* 112, 243–254.

Shaw, D.M., Munoz, G., Bottos, E.M., Duy, S.V., Sauvé, S., Liu, J., Van Hamme, J.D., **2019**. Degradation and defluorination of 6:2 fluorotelomer sulfonamidoalkyl betaine and 6: 2 fluorotelomer sulfonate by Gordonia sp. strain NB4-1Y under sulfur-limiting conditions. *Sci. Total Environ.* 647, 690–698.

Shi, Y., Vestergren, R., Nost, T. H., Zhou, Z., Cai, Y., **2018**. Probing the differential tissue distribution and bioaccumulation behavior of per-and polyfluoroalkyl substances of varying chain-lengths, isomeric structures and functional groups in crucian carp. *Environ. Sci. Technol.* 52, 4592–4600.

Simcik, M.F., Dorweiler, K.J., **2005**. Ratio of Perfluorochemical Concentrations as a Tracer of Atmospheric Deposition to Surface Waters. *Environ. Sci. Technol.* 39, 8678–8683.

Sottolichio, A., Castaing, P., **1999**. A synthesis on seasonal dynamics of highly-concentrated structures in the Gironde estuary. *C.R. Acad. Sci.* Sér. II Fasc.A-Sci. Terre Planètes 329, 795–800.

Tapie, N., **2006**. Contamination des écosystèmes aquatiques par les PCB et PBDE : Application à l'estuaire de la Gironde. PhD thesis.

Tokranov, A.K., Nishizawa, N., Amadei, C.A., Zenobio, J.E., Pickard, H.M., Allen, J.G., Vecitis, C.D., Sunderland, E.M., **2018**. How Do We Measure Poly-and Perfluoroalkyl Substances (PFASs) at the Surface of Consumer Products?. *Environ. Sci. Technol. Lett.* 6, 38–43.

Tomy, G.T., Budakowski, W., Halldorson, T., Helm, P.A., Stern, G.A., Friesen, K. Pepper, K., Tittlemier, S.A., Fisk A.T., **2004**. Fluorinated organic compounds in an eastern arctic marine food web. *Environ. Sci. Technol.* 38, 6475–6481.

Wang, Z., Boucher, J.M., Scheringer, M., Cousins, I.T., Hungerbühler, K., **2017**. Toward a comprehensive global emission inventory of C4–C10 perfluoroalkanesulfonic acids (PFSAs) and related precursors: focus on the life cycle of C8-based products and ongoing industrial transition. *Environ. Sci. Technol.* 51, 4482–4493.

Xu, J., Guo, C.S., Zang, Y., Meng, W., **2014**. Bioaccumulation and trophic transfer of perfluorinated compounds in a eutrophic freshwater food web. *Environ. Pollut.* 184, 254–261.

Yeung, L.W.Y., Dassuncao, C., Mabury, S.A., Sunderland, E.M., Zhang, X., Lohmann, R., **2017**. Vertical Profiles, Sources and Transport of PFASs in the Arctic Ocean. *Environ. Sci. Technol.* 51, 6735–6744.

Zhao, Z., Xie, Z., Tang, J., Sturm, R., Chen, Y., Zhang, G., Ebinghaus, R., **2015**. Seasonal variations and spatial distributions of perfluoroalkyl substances in the rivers Elbe and lower Weser and the North Sea. *Chemosphere*, *129*, 118–125.

Zhang, S., Lu, X., Wang, N., Buck, R.C., **2016**. Biotransformation potential of 6: 2 fluorotelomer sulfonate (6: 2 FTSA) in aerobic and anaerobic sediment. *Chemosphere* 154, 224–230.

Zhang, Y., Meng, W., Guo, C., Xu, J., Yu, T., Fan, W., Li, L., **2012**. Determination and partitioning behavior of perfluoroalkyl carboxylic acids and perfluorooctanesulfonate in water and sediment from Dianchi Lake, China. *Chemosphere* 88, 1292–1299.

Table 1. Summary of PFAS detection frequencies (%) and concentrations (ng L^{-1}) in surface water samples from the present survey (dissolved phase). Compounds that were not detected are not shown.

	Detection Frequency	Concentration range*
	%	ng L^{-1}
PFBA	50	0.39–2.0
PFPeA	100	0.26–2.4
PFHxA	100	0.46–2.0
PFHpA	100	0.24–1.4
PFOA	100	0.40–1.9
PFNA	100	0.09–0.27
PFDA	100	0.06–0.22
PFUnDA	50	0.02–0.04
PFBS	100	0.26–0.69
PFHxS	100	0.58–1.3
PFHpS	92	0.02–0.07
Br-PFOS	100	0.23–0.79
L-PFOS	100	0.25–0.80
ΣPFOS**	100	0.48–1.6
FOSA	75	0.01–0.05
6:2 FTSA	75	0.05–0.52

*Min-max of samples >LOD. **Sum of branched and linear isomers.

Table 2. Summary of field-based partitioning coefficients determined at Pauillac (mean ± standard deviation), including SPM-derived Log K_D and Log K_{OC} partitioning coefficients, as well as bioaccumulation factors (BAF) and biota to suspended solid accumulation factors (BSSAF).

	SPM-water		***Copepoda, ind.***		***Mysidacea, ind.***		***Palaemon longirostris***		***Crangon crangon***	
	Log K_D	**Log K_{OC}**	**Log BAF**	**BSSAF**	**Log BAF**	**BSSAF**	**Log BAF**	**BSSAF**	**Log BAF**	**BSSAF**
PFHpA	2.0 ± 0.4	3.7 ± 0.4	2.5 ± 0.2	2.4	-	-	-	-	-	-
PFOA	2.4 ± 0.2	4.1 ± 0.2	2.5 ± 0.2	1.2 ± 0.7	2.5	1.7	2.3 ± 0.2	0.7 ± 0.3	2.5 ± 0.3	1.1 ± 0.4
PFNA	2.9 ± 0.2	4.6 ± 0.2	2.8 ± 0.2	0.7 ± 0.3	2.9 ± 0.2	1.1 ± 0.6	2.9 ± 0.3	1.0 ± 0.6	3.7 ± 0.3	4.3 ± 1.4
PFDA	3.4 ± 0.2	5.1 ± 0.2	3.3 ± 0.2	0.9 ± 0.8	3.5 ± 0.3	1.3 ± 0.7	3.3 ± 0.2	0.8 ± 0.4	4.0 ± 0.3	4.6 ± 2.7
PFUnDA	3.8 ± 0.3	5.4 ± 0.3	3.7 ± 0.2	1.2 ± 1.0	3.7 ± 0.3	1.1 ± 0.6	3.7 ± 0.2	1.0 ± 0.5	4.1 ± 0.2	4.0 ± 1.9
PFDoDA	-	-	-	1.0 ± 0.3	-	1.6 ± 0.6	-	2.2 ± 0.8	-	3.4 ± 1.5
PFTrDA	-	-	-	2.3	-	2.8 ± 0.4	-	4.6 ± 2.2	-	4.8 ± 1.8
PFTeDA	-	-	-	-	-	-	-	3.8	-	-
PFHxS	1.9 ± 0.3	3.7 ± 0.3	2.0 ± 0.2	1.3 ± 0.9	1.9 ± 0.4	0.9 ± 0.5	1.9 ± 0.2	1.1 ± 0.7	2.4 ± 0.2	4.1 ± 2.8
PFHpS	2.6 ± 0.2	4.3 ± 0.3	3.1	-	3.2 ± 0.3	-	2.9 ± 0.2	-	3.3 ± 0.1	-
Br-PFOS	3.0 ± 0.3	4.7 ± 0.2	2.7 ± 0.2	0.7 ± 0.3	3.1 ± 0.2	1.5 ± 0.8	2.4 ± 0.2	0.3 ± 0.2	3.0 ± 0.1	1.4 ± 0.4
L-PFOS	3.4 ± 0.2	5.0 ± 0.2	3.4 ± 0.2	1.4 ± 0.9	3.9 ± 0.2	3.8 ± 2.2	3.4 ± 0.2	1.2 ± 0.7	3.9 ± 0.1	4.6 ± 1.9
EtFOSAA	-	-	-	1.1 ± 0.5	-	0.9	-	1.9 ± 1.3	-	1.9 ± 1.6
L-FOSA	3.5 ± 0.2	5.3 ± 0.2	4.1 ± 0.4	4.8 ± 3.8	4.9 ± 0.2	20 ± 11	4.8 ± 0.3	21 ± 11	5.0 ± 0.4	29 ± 9
MeFOSA	-	-	-	3.1	-	-	-	-	-	-
6:2 FTSA	2.4 ± 0.2	4.0 ± 0.2	-	-	-	-	-	-	-	-

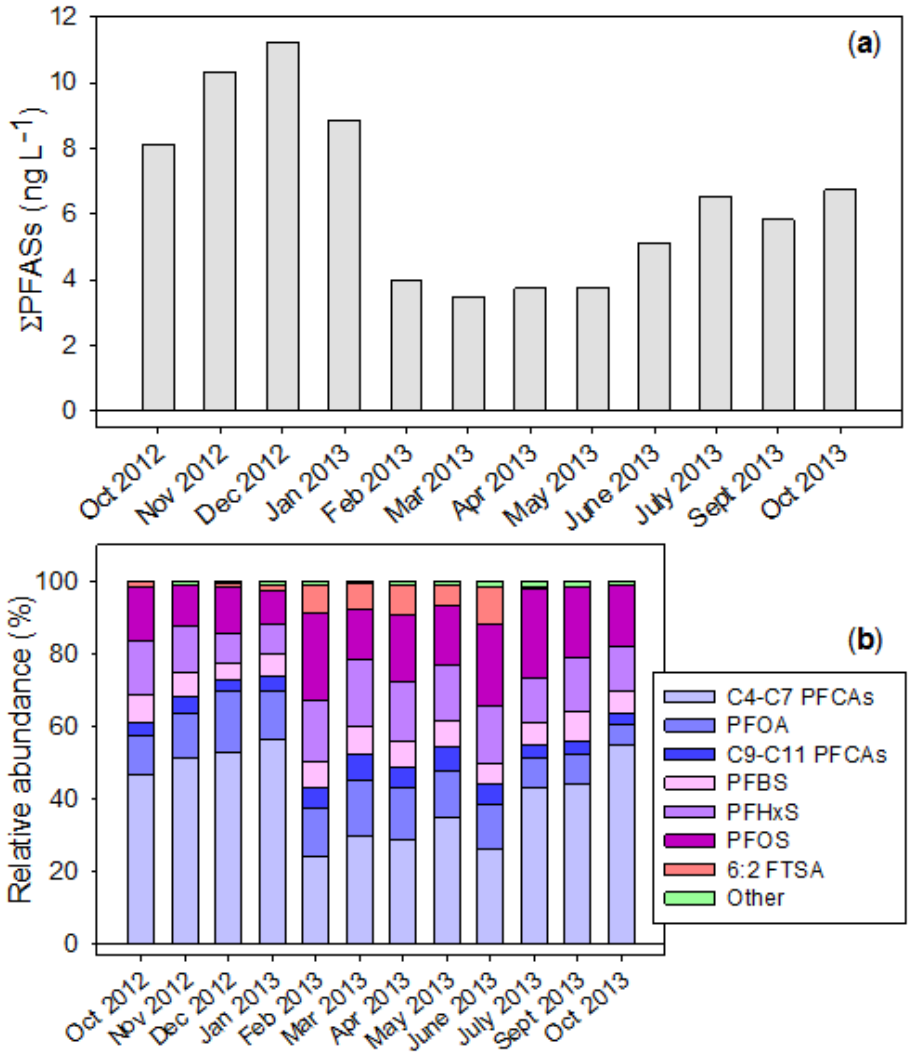

Figure 1. Seasonal variations of ΣPFASs in the dissolved phase (**a**) and corresponding composition profiles (relative abundance, in % of ΣPFASs) (**b**) observed at Pauillac (Gironde estuary).

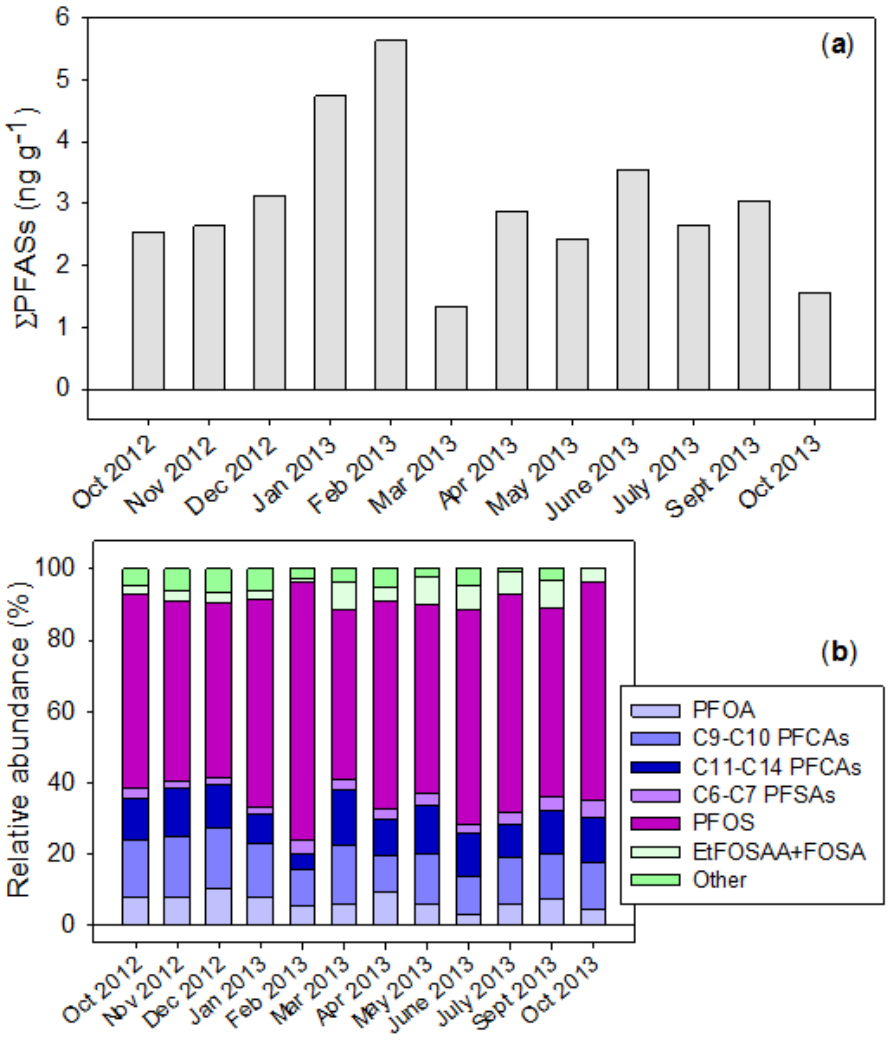

Figure 2. Seasonal variations of ΣPFASs in the suspended sediment (**a**) and corresponding composition profiles (relative abundance, in % of ΣPFASs) (**b**) observed at Pauillac (Gironde estuary).

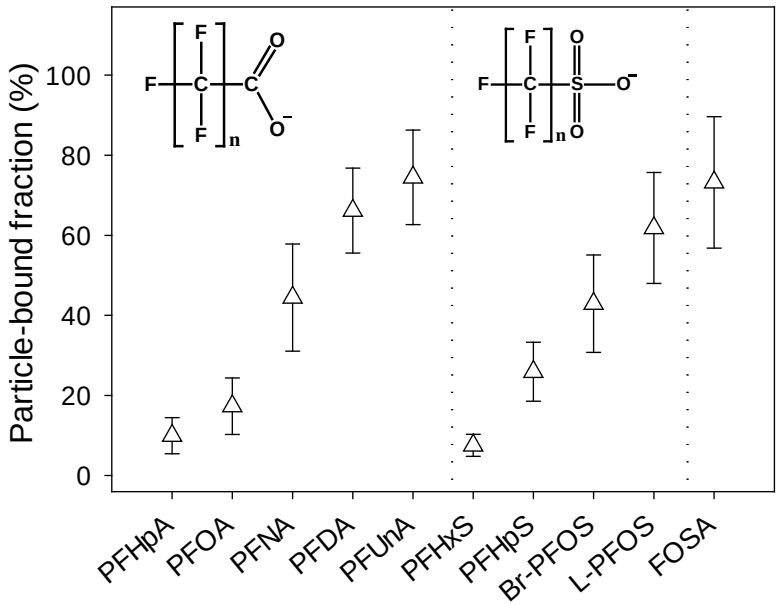

Figure 3. Average particle-related fraction (φ = ratio of the PFAS concentration determined in the SPM to that determined in the water, i.e., dissolved + SPM) for PFCAs, PFSAs, FOSA and 6:2 FTSA. Error bars represent standard deviations.

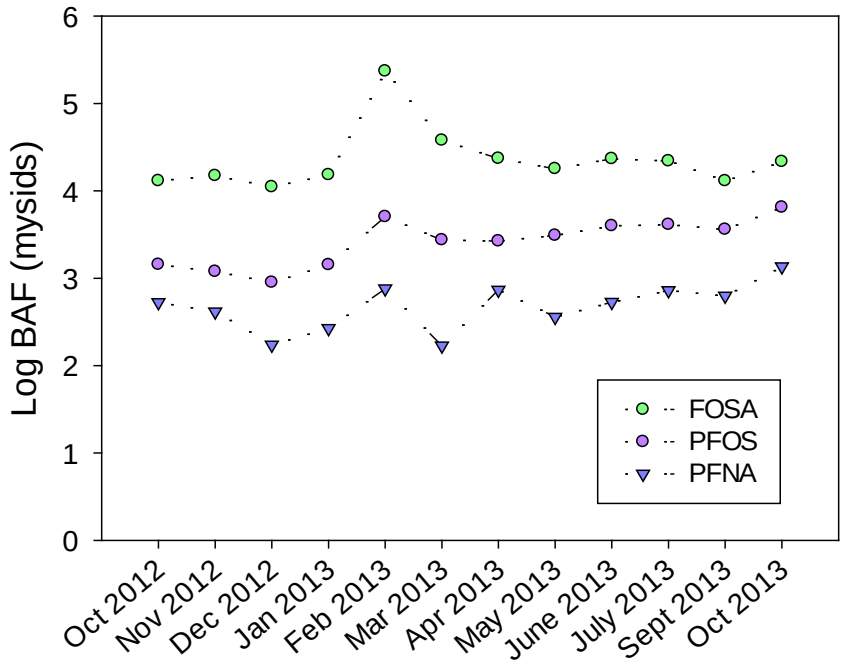

Figure 4. Variations of the bioaccumulation factor (Log BAF = C_{biota}/C_{water}) illustrated in the case of mysids for perfluorooctane sulfonamide (FOSA), perfluorooctane sulfonate (L-PFOS), and perfluorononanoate (PFNA).